Power Allocation for Distributed Antenna Systems in Frequency-Selective Fading Channels

Qi-Yue Yu, *Member, IEEE*, Ya-Tian Li, Wei Xiang, *Senior Member, IEEE*, Wei-Xiao Meng, *Senior Member, IEEE*, and Wen-Yan Tang

***Abstract*—A distributed antenna system (DAS) is very attractive, since it can reduce transmit power by shortening the distance between antenna elements (AEs) and the mobile station. This paper investigates the channel capacity of the DAS over a multi-path frequency-selective fading channel. We first show that the optimal power allocation solution to approaching the channel capacity is unrealistic for the practical DAS. Then, a near-optimal scheme is given through maximally tightening the upper bound of the channel capacity. Approximate analytical results are obtained through the use of the central-limit theorem. Both simulation and theoretical results are presented to show that the channel capacity can be greatly enhanced by the proposed power allocation schemes. Moreover, the bit error rate performance is analyzed for the proposed scheme.**

***Index Terms*—Distributed antenna system (DAS), channel capacity, power allocation, frequency-selective fading channel, central-limit theorem.**

I. Introduction

RECENTLY, energy-efficient wireless networks becomes very popular for the fifth generation (5G) cellular systems, which aims to significantly increase data rates with comparatively low transmit power [1]–[3]. How to improve energy efficiency (EE) while simultaneously achieving good spectrum efficiency (SE) performance is one of the most popular research topics for 5G [1].

In the past decades, the distributed antenna system (DAS) has attracted considerable attention. The essence behind the DAS is that several antenna elements (AEs) are geographically distributed in a service cell, and connected to a signal processing center through dedicated links such as optic fibres. A DAS can be thought of as a distributed multiple antennas system. A mobile station (MS) in the service area can communicate with one or more AEs, which helps reduce the transmit power greatly due to the shortened transmission distance [4]–[6]. Moreover, spectral efficiency can be improved thanks to multi-antenna transmission.

One of popular research topics on DAS is to investigate its channel capacity–[21]. Some papers in the literature focus on the capacity of different DAS structures. For example, the authors in [8] discuss the capacity of the DAS with linear block precoding, while the authors in [10] focuse on the DAS channel capacity through space-time block coded diversity.

On the other hand, some researchers investigate the channel capacity of the DAS under different channel environments. For instance, the DAS capacity in a slow fading channel is investigated in [13], while the authors in [11] discuss the capacity of the downlink DAS with sectionized antennas under the time-varying frequency-selective fading channel. The capacity of the DAS in generalized-K fading channels is investigated in [15]. Moreover, the authors in [9] investigate the cell average ergodic capacity of the DAS using a composite fading channel model at high signal-to-noise ratios (SNRs). A closed-form expression of the channel capacity for the downlink DAS with a known MS distribution is derived in [12]. The authors in [16] investigate the multiple-access channel problem, while the authors in [17] discuss cooperative transmission.

Power allocation plays an important role in improving the channel capacity of the DAS. A large number of studies in the literature have been dedicated to this issue [22]–[27]. For example, some power allocation schemes for the multi-cell case are proposed in [22], [23]. The authors in [25] and [26] investigate power allocation for both the DAS with a random antenna layout and the generalized DAS. A power allocation scheme with a minimum bit error rate (BER) constraint in a slow-vary fading channel is investigated in [24]. In [27], power allocation for the DAS considers multicast Quality of Service (QoS) guarantees. In [28], optimal precoding and power/bit allocation for the multiple-input-single-output (MISO) channel is studied. However, no power allocation can be optimal if the phase of the channel condition is unknown at the transmitter. The authors of [29] present an optimal power allocation scheme for EE maximization in DAS, and derive a closed-form optimal solution. The work in [30] focuses on the problem of optimal antenna selection and power allocation for downlink DAS to maximize EE. A low-complexity power allocation algorithm aiming at maximizing EE is proposed in [31]. In [35], the authors investigate the problem of power allocation for downlink joint user

Manuscript received May 6, 2015; revised October 9, 2015; accepted November 22, 2015. Date of publication December 3, 2015; date of current version January 14, 2016. This work was supported in part by the National Natural Science Foundation of China under Grant 61201148, and China Postdoctoral Science Foundation funded project (Nos. 2013M540291 and 2014T70337), and in part by the Key Laboratory of Universal Wireless Communications (Beijing University of Posts and Telecommunications), Ministry of Education, China. The associate editor coordinating the review of this paper and approving it for publication was M. C. Gursoy.

Q.-Y. Yu, W.-X. Meng, and W.-Y. Tang are with Department of Communication Engineering, Harbin Institute of Technology (HIT), Harbin 150001, China (e-mail: yuqiyue@hit.edu.cn; wxmeng@hit.edu.cn; tangwy@hit.edu.cn).

Y.-T. Li is with the Changchun Institute of Optics, Fine Mechanics and Physics (CIOMP), Chinese Academy of Sciences, Changchun, China (e-mail: orcprince@126.com).

W. Xiang is with the College of Science, Technology and Engineering, James Cook University, Cairns, Qld. 4870, Australia (e-mail: wei.xiang@jcu.edu.au).

Color versions of one or more of the figures in this paper are available online at http://ieeexplore.ieee.org.

Digital Object Identifier 10.1109/TCOMM.2015.2504958

scheduling, under the assumption that the power of each AE is uniformly allocated to all the users with the same power restriction. The QoS is guaranteed through iteratively removing the user with the worst quality. The author in [36] propose an optimal power allocation scheme for the DAS in the slow fading channel using the proximal point method. The Karush-Kuhn-Tucker conditions and iterations are also used to maximize the channel capacity. It is noted that the maximal transmitted power of each AE is limited.

Resource allocation is also a topic of particular interest for the DAS. Some previous studies have proposed various resource allocation algorithms for the orthogonal frequency division multiple access (OFDMA) multiuser DAS [32], [33], and usually the multi-user scenarios increase the complexity of the allocation algorithms. The authors in [32] propose a a chunk allocation technique, which aggregates a set of contiguous sub-carriers into one chunk and then allocates resources chunk by chunk. Resource allocation for the popular ultra-dense networks based on the DAS is also a hot topic [34].

In comparison to the work in [35], [36], this paper focuses on the channel capacity of the DAS in the multi-path Rayleigh fading channel, and attempts to maximize the channel capacity under the condition that the total power of the DAS is constrained. This condition is more flexible than the one that assumes each antenna has the same power. Thus, the work can be extended to many other interesting scenarios, particularly in terms of EE discussion. Moreover, the BER performance of the OFDM-based DAS is also presented in this paper. The main contributions of this paper are three-fold: (1) a near-optimum allocation scheme for the DAS is proposed through maximizing the upper bound of the channel capacity; (2) a theoretical analysis of the near-optimal power allocation scheme is presented; and (3) bounds of the channel capacity and the corresponding BER analysis are derived.

The reminder of this paper is organized as follows. In Section II, the DAS model and its channel capacity are discussed. Section III presents our proposed power allocation schemes. A theoretical analysis of the proposed power allocation schemes is given in Section IV. In Section V, both analytical and simulated capacities, and the BERs for the proposed power allocation schemes are presented. Some concluding remarks are given in Section VI.

II. System Model

The system model adopted in this paper is illustrated in Fig. 1, where N_{AE} AEs are uniformly distributed in the area, and connected with the base station (BS) through optical fibres. The downlink DAS with a single-antenna user randomly distributed in the given area is considered. In this paper, the following notation is used: $*$ denotes the convolution of two functions, $E[\cdot]$ represents mathematical expectation, and x^+ is defined as $x^+ = max\{0, x\}$.

Fig. 2 depicts a block diagram to illustrate the signal flow of the transceiver. For the downlink DAS, each distributed antenna can be viewed as a transmitter. The OFDM technique is employed for the proposed scheme. It is noted that the same data are transmitted on the same sub-carriers from all N_{AE} AEs, and different data sequences are sent on different subcarriers.

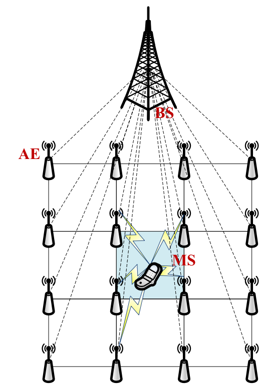

Fig. 1. DAS topology model, where the AEs are connected with the BS through optical fibres.

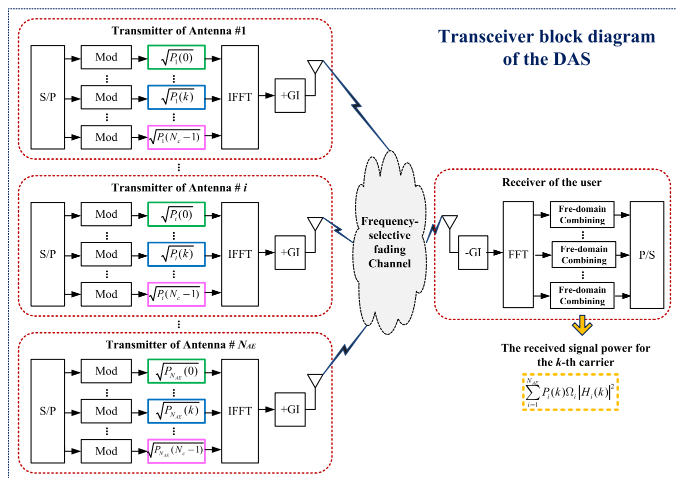

Fig. 2. Transceiver block diagram of the DAS, where "Mod" indicates modulation, "S/P" and ""P/S" stand for serial-to-parallel and parallel-to-serial, "+GI" and "-GI" represent the addition and removal of the guard interval, respectively.

Hence, diversity (for the same sub-carrier) is achieved by using all the AEs, while multiplexing is obtained via differing sub-carriers. It should be noted that, since the AEs are located in different places, the signals from the AEs cannot arrive at the mobile station simultaneously, resulting in multiple-access interference (MAI). A great deal of research has been undertaken on the MAI problem, *e.g.*, multi-user detection (MUD), block spread CDMA [37] etc. Therefore, this paper assumes that MAI can be completely eliminated by some popular MUD (or block spread CDMA) techniques.

The transmit signal from the i-th AE is defined as $s_i(t)(i = 1, 2, \ldots, N_{AE})$, and the corresponding transmit power is denoted by P_i. The total transmit power satisfies $P = \sum_{i=1}^{N_{AE}} P_i$, where P is the total transmit power.

The received signal $r(t)$ at the receiver is given by

$$r(t) = \sum_{i=1}^{N_{AE}} \left[\left(\sqrt{\Omega_i} h_i(t) \right) * \left(\sqrt{P_i} s_i(t) \right) \right] + n(t), \quad (1)$$

where $n(t)$ is the additive white Gaussian noise (AWGN) with variance σ_n^2, and Ω_i is related to the path loss and shadowing of the i-th AEs, given by

$$\Omega_i = d_i^{-\alpha} 10^{\frac{\eta_i}{10}}, \quad (2)$$

where d_i is the normalized distance between the i-th AE and the mobile user, α is the pass loss exponent, and η_i is a zero-mean Gaussian random variable with standard deviation σ_i in dB.

In (1), $h_i(t)$ is the channel impulse response between the i-th AE and the MS, which is composed of maximum L chip-spaced independent paths expressed as

$$h_i(t) = \sum_{l=0}^{L-1} h_{i,l}\delta(t - \tau_{i,l}), \tag{3}$$

where $h_{i,l}$ and $\tau_{i,l}$ are the complex-valued path gain and the time delay of the l-th path from the i-th AE to the user, respectively. Let $H_i(k)(k = 0, \ldots, N_c - 1)$ be the channel frequency response of the k-th sub-carrier of the i-th AE, given as

$$H_i(k) = \frac{1}{\sqrt{N_c}} \sum_{l=0}^{L-1} h_{i,l} \exp\left(-j2\pi k \frac{l}{N_c}\right), \tag{4}$$

where N_c is the size of the discrete Fourier transform (DFT). Denote by $\Pi(k)$ the Gaussian noise $n(t)$ in frequency-domain form, and it is easy to infer that the variance of $\Pi(k)$ equates to σ_n^2.

Suppose that $P_i(k)$ is the amount of power allocated to the k-th subcarrier of the i-th AE, which satisfies

$$P = \sum_{i=1}^{N_{AE}} \sum_{k=0}^{N_c-1} P_i(k). \tag{5}$$

At the MS, $\gamma_i(k)$ is denoted as the received signal-to-noise ratio (SNR) at the i-th AE of the k-th subcarrier, which can be expressed as

$$\gamma_i(k) = \frac{1}{\sigma_n^2}\left(P_i(k)\Omega_i|H_i(k)|^2\right). \tag{6}$$

Thereby, the channel capacity can be derived as

$$\begin{aligned} C &= \sum_{k=0}^{N_c-1} \log_2\left(1 + \sum_{i=1}^{N_{AE}} \gamma_i(k)\right) \\ &= \sum_{k=0}^{N_c-1} \log_2\left(1 + \sum_{i=1}^{N_{AE}} P_i(k) y_i\,(k)\right), \end{aligned} \tag{7}$$

where $y_i\,(k)$ is equal to $\left(\Omega_i|H_i(k)|^2\right)/\sigma_n^2$, which measures the channel condition and the noise between the i-th AE and the k-th subcarrier at the receiver.

According to (7), to maximize the channel capacity C, the key is to find the optimum power allocation scheme for $P_i\,(k)$. Towards this end, we utilize the standard Lagrange multipliers' method. Given the objective function in (7) and constraint function $P = \sum_{i=1}^{N_{AE}} P_i$, the Lagrange function F_1 can be written as

$$\begin{aligned} F_1 = &\sum_{k=0}^{N_c-1} \log_2\left(1 + \sum_{i=1}^{N_{AE}} y_i(k)P_i(k)\right) \\ &- v\left(\sum_{i=1}^{N_{AE}} \sum_{k=0}^{N_c-1} P_i(k) - P\right), \end{aligned} \tag{8}$$

where v is the Lagrange multiplier, $y_i(k)$ is positive for $i = 1, \ldots, N_{AE}$, and $P_i(k)(1 \le i \le N_{AE}, 1 \le k \le N_c)$ are the roots.

To maximize (7), the partial derivative of the left hand side of (8) should be set to zero. It follows that

$$\frac{\partial F_1}{\partial P_m(k_0)} = \frac{1}{\ln 2} \frac{y_m(k_0)}{1 + \sum_{i=1}^{N_{AE}} y_i(k_0) \cdot P_i(k_0)} - v = 0 \tag{9}$$

where $m(1 \le m \le N_{AE})$ is an integer, and an arbitrary k_0 satisfies $0 \le k_0 \le N_c - 1$.

It is easy to learn that (9) has the same roots, independent of the value of m. This means that for any arbitrary m $(1 \le m \le N_{AE})$, $y_m(k)$ is deterministic given k. However, this is impossible for the practical DAS, since the spatial distances between each AE and the user cannot be identical. Thus, one cannot find the optimal power solutions by using the Lagrange multipliers' method.

III. Power Allocation Schemes

Since the optimal numerical solution is not attainable, near-optimal solutions are proposed in this section. We first derive a upper bound expression for the channel capacity, and then present a power allocation scheme to approach the derived upper bound.

A. Preliminaries

Before proposing our power allocation schemes, we first give two lemmas, the proofs of which are detailed in Appendix.

Lemma 1: Suppose $a_i > 0$ for any positive integer i. It can be shown that

$$\begin{aligned} \prod_{i=1}^{n}(1 + a_i) =&(1 + \sum_{i_1=1}^{n} a_i + \sum_{i_1 \ne i_2}^{n} a_{i_1}a_{i_2} + \cdots \\ &+ \sum_{i_1 \ne i_2 \ne \cdots i_n}^{n} a_{i_1}a_{i_2}\cdots a_{i_n}), \end{aligned} \tag{10}$$

where i_k is a positive integer satisfying $1 \le i_k \le n$ for any integer k.

Lemma 2: Suppose $a_i > 0$ for any positive integer i. It can be shown that

$$\log_2(1 + \sum_{i=1}^{n} a_i) < \sum_{i=1}^{n} \log_2(1 + a_i). \tag{11}$$

From Lemma 2, a upper bound C_{up} and a lower bound C_{low} of the channel capacity in (7) can be derived as

$$\begin{cases} C \leqslant C_{up} = \sum\limits_{k=0}^{N_c-1} \sum\limits_{i=1}^{N_{AE}} \log_2\left(1 + \gamma_i(k)\right) \\ C \geqslant C_{low} = \log_2\left(1 + \sum\limits_{k=0}^{N_c-1} \sum\limits_{i=1}^{N_{AE}} \gamma_i(k)\right). \end{cases} \tag{12}$$

It is easy to show that C_{up} and C_{low} are the channel capacities of the full-multiplexing scheme and full-diversity scheme, respectively.

B. Capacity Bounds

Denote by δ_{up} and δ_{low} the difference between C_{up} and C, and the difference between C_{low} and C, respectively.

Apparently, δ_{up} can be written as

$$\begin{aligned}\delta_{up} &= C_{up} - C \\ &= \sum_{k=0}^{N_c-1}\left\{\log_2\left[\prod_{i=1}^{N_{AE}}(1+\gamma_i(k))\right] - \log_2\left(1+\sum_{i=1}^{N_{AE}}\gamma_i(k)\right)\right\}.\end{aligned} \tag{13}$$

Due to Lemma 1, δ_{up} can be further simplified as follows

$$\begin{aligned}\delta_{up} = \sum_{k=0}^{N_c-1}\log_2\Bigg\{1+\Bigg[\sum_{i_1\neq i_2}^{N_{AE}}\gamma_{i_1}(k)\,\gamma_{i_2}(k) + \cdots + \\ \sum_{i_1\neq i_2\neq\cdots i_{N_{AE}}}^{N_{AE}}\gamma_{i_1}(k)\cdots\gamma_{i_{N_{AE}}}(k)\Bigg]\Big/\left[1+\sum_{i=1}^{N_{AE}}\gamma_i(k)\right]\Bigg\},\end{aligned} \tag{14}$$

where i_l is a positive integer satisfying $1 \leq i_l \leq N_{AE}$ for any integer l. Let ρ_{up} be

$$\begin{aligned}\rho_{up} = \Bigg\{\sum_{i_1\neq i_2}^{N_{AE}}\gamma_{i_1}(k)\,\gamma_{i_2}(k) + \cdots + \\ \sum_{i_1\neq i_2\neq\cdots i_{N_{AE}}}^{N_{AE}}\gamma_{i_1}(k)\,\gamma_{i_2}(k)\cdots\gamma_{i_{N_{AE}}}(k)\Bigg\}\cdot\frac{1}{1+\sum_{i=1}^{N_{AE}}\gamma_i(k)}.\end{aligned} \tag{15}$$

Thus, the channel capacity C approaches its upper bound C_{up} when ρ_{up} can be approximated to zero. If $\gamma_i(k)$ meets the condition that $\gamma_i(k) < 1$ for every $0 \leq i \leq N_{AE}$, the higher order product terms in the numerator of (15) are negligible. As a result, ρ_{up} approximately equates to zero.

In a similar way, it follows that

$$\begin{aligned}\delta_{low} &= C - C_{low} \\ &= \log_2\left[\prod_{k=0}^{N_c-1}\left(1+\sum_{i=1}^{N_{AE}}\gamma_i(k)\right)\right] \\ &\quad - \log_2\left(1+\sum_{i=1}^{N_{AE}}\sum_{k=0}^{N_c-1}\gamma_i(k)\right).\end{aligned} \tag{16}$$

Letting $\alpha(k) = \sum_{i=1}^{N_{AE}}\gamma_i(k)$ and using Lemma 1, δ_{low} can be simplified to

$$\begin{aligned}\delta_{low} = \log_2\Bigg\{1+\Bigg[\sum_{k_1\neq k_2}^{N_c}\alpha(k_1)\,\alpha(k_2) + \cdots + \\ \sum_{k_1\neq k_2\neq\cdots k_{N_c}}^{N_c}\alpha(k_1)\cdots\alpha_{k_c}(k_{N_c})\Bigg]\Big/\left[1+\sum_{i=1}^{N_c}\alpha(k)\right]\Bigg\}.\end{aligned} \tag{17}$$

Due to the same reason as in the case of the upper bound, the channel capacity approaches its lower bound when the ratio term in (17) is close to zero, implying $\alpha(k) = \sum_{i=1}^{N_{AE}}\gamma_i(k) < 1$. It will be proved in Section IV that this lower bound is very loose.

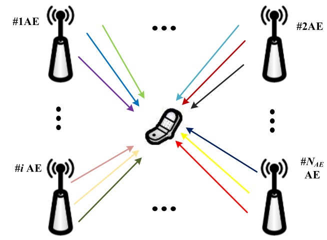

Fig. 3. System block diagram when $C = C_{up}$.

Actually, both the upper and lower bounds represent two special cases of the DAS. For the upper bound C_{up}, the system can be viewed as a parallel transmission system shown in Fig. 3 with $N_c N_{AE}$ parallel carriers, where y_i' are all the elements in (24) for any integer i $(1 \leq i \leq N_{AE}N_c)$, indicating the channel conditions of the parallel transmission system. p_i' is the power allocated to the i-th subcarrier corresponding to y_i'. This system is a full-multiplexing one.

Summarily, when $C = C_{low}$, it implies that the DAS has only one carrier, and the order of diversity is $N_c N_{AE}$. The system model is similar to Fig. 1, but the spatial diversity gain is $N_c N_{AE}$. This system becomes a full diversity one.

C. Power Allocation Scheme

As discussed above, the channel capacity approaches its upper bound C_{up} when $\gamma_i(k) < 1$. However, this condition may not be met when the total power P is large enough. In the following section, we will prove that, in general cases, $y_i(k)$ is usually small enough to satisfy the constraint of $\gamma_i(k) < 1$.

Since there exist no optimal solutions to (7) for practical DAS systems, our strategy is to maximize the channel capacity by maximizing its upper bound. We still utilize the Lagrange multipliers method to derive a near-optimal power allocation scheme. The following Lagrange function F_2 is given as

$$\begin{aligned}F_2 = &\sum_{i=1}^{N_{AE}}\sum_{k=0}^{N_c-1}\log\left(1+y_i(k)P_i(k)\right) \\ &- v\left(\sum_{i=1}^{N_{AE}}\sum_{k=0}^{N_c-1}P_i(k) - P\right).\end{aligned} \tag{18}$$

Compared with F_1 in (8), the object function is modified according to the upper bound. For an arbitrary i_0-th AE $(1 \leq i_0 \leq N_{AE})$ and k_0-th subcarrier $(1 \leq k_0 \leq N_c)$, the partial derivatives of (18) ought to be zeros

$$\frac{\partial F_2}{\partial P_{i_0}(k_0)} = \frac{1}{\ln 2}\cdot\frac{y_{i_0}(k_0)}{1+P_i(k_0)} - v = 0. \tag{19}$$

It is easy to show that the solution to (19) is

$$P_{i_0}(k_0) = \left(\lambda - \frac{1}{y_{i_0}(k_0)}\right)^+, \tag{20}$$

where λ is equal to $1/v$.

For mathematical convenience, we denote by Ψ the set of all the subcarriers of the DAS as follows

$$\Psi := \{(i,k)\,|i = 1, 2 \cdots, N_{AE}; k = 0, 1, 2, \cdots, N_c - 1\}. \tag{21}$$

Let Ψ_u be the set of the subcarriers used in the allocation scheme, which is defined as

$$\Psi_u := \{(i,k)\,|P_i(k) > 0, (i,k) \in \Psi\}. \tag{22}$$

It is easy to see that $\Psi_u \subseteq \Psi$.

Denote by $\overline{\Psi}_u$ the complement of Ψ_u, and let N_Ψ and N_{Ψ_u} be the cardinals of Ψ and Ψ_u, respectively.

According to (6) and (20), λ can be derived as

$$\lambda = \frac{P}{N_{\Psi_u}} + \sum_{(i,k)\in\Psi_u} \frac{1}{y_i\,(k)}. \tag{23}$$

Combining (20) and (23) gives rise to a near-optimal scheme. This method views the channel state information (CSI) of all the antennas as a matrix given below

$$Y = \begin{bmatrix} \Omega_1 H_1(0)^2 & \cdots & \Omega_{N_{AE}} H_{N_{AE}}(0)^2 \\ \vdots & \ddots & \vdots \\ \Omega_1 H_1(N_c-1)^2 & \cdots & \Omega_{N_{AE}} H_{N_{AE}}(N_c-1)^2 \end{bmatrix}^T. \tag{24}$$

where Y indicates the channel conditions of all the subcarriers from each AE to the MS.

Hence, there are $N_{AE}N_c$ instead of $N_{AE}L$ channel impulses. The proposed power allocation scheme is derived as follows. If all the $N_{AE}N_c$ elements in Y are ordered in descending order, the first N_{Ψ_u} subcarriers will be allocated power, whereas the remaining subcarriers receive zero power. To summarize, the proposed power allocation scheme can be mathematically expressed as

$$P_{i_0}\,(k_0) = \begin{cases} \frac{P}{N_{\Psi_u}} + \sum\limits_{\substack{(i,j)\in\Psi_u \\ (i,j)\neq(i_0,j_0)}} \frac{\sigma_n^2}{\Omega_i |H_i(k)|^2} & , (i_0, j_0) \in \Psi_u \\ 0 & , (i_0, j_0) \in \Psi/\Psi_u \end{cases}, \tag{25}$$

where Ψ/Ψ_u represents the difference set between Ψ and Ψ_u. The intuition of this power allocation scheme is to allocate more power to the better channels.

IV. Theoretical Analysis

This section presents a theoretical analysis of the above power allocation methods. A key step is to derive the expectation of the channel capacity. After revealing that it is impractical to achieve an exact solution, the Central-Limit Theorem is resorted to obtain an approximate solution. Towards the end of this section, some further discussions are provided.

A. Accurate Theoretical Analysis

This part aims to derive an accurate value for the expected channel capacity by integrals. Considering $|H_i(k)|^2$ and Ω_i are independent, the average channel capacity in (7) can be shown as

$$E\,(C) = \int_0^{+\infty} \int_0^{+\infty} C \prod_{i=1}^{N_{AE}} f_{|H_i(k)|^2}\left(|H_i(k)|^2\right) f_\Omega\,(\Omega_i) \cdot \prod_{i=1}^{N_{AE}} d\Omega_i \prod_{k=0}^{N_c-1} d\left(|H_i(k)|^2\right), \tag{26}$$

where C is equal to $\sum\limits_{k=0}^{N_c-1} \log_2\left(1 + \sum\limits_{i=1}^{N_{AE}} P_i(k)|H_i\,(k)|^2\Omega_i\right)$. And $f_{|H_i(k)|^2}\left(|H_i(k)|^2\right)$ and $f_\Omega\,(\Omega_i)$ are the PDFs of $|H_i(k)|^2$ and Ω_i respectively, which are discussed below.

As it is well known, the real and imaginary components of $h_{i,l}$ are independent identical distribution (i.i.d) Gaussian distributed, so that, $|h_{i,l}|$ follows a Rayleigh distribution. On the ground that the DFT coefficients of complex Gaussian variables are still Gaussian distributed, it is easy to see that $H_i(k)$ follows a complex Gaussian distribution. Thus the PDF of $|H_i(k)|^2$ follows a chi-square distribution with two degrees of freedom, with its PDF given by

$$f_{|H_i(k)|^2}\left(|H_i(k)|^2\right) = \begin{cases} N_c \exp(-N_c|H_i(k)|^2) & , |H_i(k)|^2 \geq 0 \\ 0 & , |H_i(k)|^2 < 0 \end{cases}. \tag{27}$$

Since η_i is a zero-mean Gaussian random variable with standard deviation σ, the PDF $f_\Omega\,(\Omega)$ is given as

$$f_\Omega\,(\Omega_i) = \frac{1}{\sqrt{2\pi}\sigma} \exp\left(-\frac{100\lg^2(\Omega_i)}{2\sigma^2}\right), \tag{28}$$

where Ω_i is set to $d_i^{-\alpha}10^{0.1\times\eta_i}$, and the $d_i^{-\alpha}$ is considered as a constant.

As can be inferred from (26) there are N_{AE} nested integrals for Ω_i $(i = 1, \ldots, N_{AE})$, and $N_{AE}N_c$ nested integrals for $|H_i(k)|^2$ $(k = 1, \ldots, N_C)$. Thus, a total of $(N_c + 1)N_{AE}$ nested integrals are required. This resulting complexity is intractable for deriving analytical solutions. Moreover, even the Monte Carlo method is difficult to obtain numerical solutions. Thus, how to analytically obtain approximate solutions is a challenging problem.

It is noted that the channel capacity can be approximated by its upper bound in (12), which indicates the approximated channel capacity C is determined by $\gamma_i(k)$. Considering $\gamma_i(k) = \frac{1}{\sigma_n^2}\left(P_i(k)\Omega_i|H_i(k)|^2\right)$, it is able to show that $\gamma_i(k)$ is determined when $P_i(k)$ and $y_i(k)$ are both constants. Since $y_i(k)$ equals $\left(\Omega_i|H_i(k)|^2\right)/\sigma_n^2$, the expectation $E\,(y_i\,(k))$ can be derived from the joint distribution of Ω_i and $|H_i(k)|^2$. That is, $E\,(y_i\,(k))$ is obtained by a double integral of Ω_i, $|H_i(k)|^2$ and their PDFs. Due to the inter-dependence of Ω_i and $|H_i(k)|^2$, $E\,(y_i\,(k))$ can be simplified as

$$E\,(y_i\,(k)) = \frac{1}{\sigma_n^2} \int_0^{+\infty} \int_0^{+\infty} |H_i(k)|^2\Omega_i f_{|H_i(k)|^2}\left(|H_i(k)|^2\right) \cdot f_\Omega\,(\Omega_i)\, d\Omega_i d|H_i(k)|^2. \tag{29}$$

It is noted that the expectation of σ_n^2 is a constant. Through computer simulations, it is shown that $E(y_i(k))$ equals 0.0426 under the simulation conditions given in Table I, which ensures that $\gamma_i(k)$ is almost always smaller than 1, and can be verified by the results in Table II. It should be noted that the received SNR is influenced by the path loss, shadowing, the channel condition and the noise power between the i-th AE and the user terminal. Letting $\sum_{l=0}^{L-1} |h_{i,l}|^2 = 1$ makes the average channel gain to be 1. Moreover, it is known that $E(|H_i(k)|^2) = \frac{1}{N_c}$, when $N_c >> 1$, so that $E(|H_i(k)|^2) << 1$. Considering the distance d_i between the user and i-th AE is normalized to be 1 in the simulation, it can be derived that $\gamma_i(k) < 1$, so that this important assumption holds $\gamma_i(k)$ is not greater than 1. After proving $\gamma_i(k) < 1$, the expectation $E(C)$ of the channel capacity can be simplified by its upper bound, *i.e.*,

$$E(C) \approx E\left(\sum_{i=1}^{N_{AE}} \sum_{k=0}^{N_c-1} \log_2(1 + \gamma_i(k))\right). \tag{30}$$

Note that $\log(1 + \gamma_i(k))$ is equal to zero, when (i, k) belongs to $\overline{\Psi}_u$. Then (30) can be further simplified into

$$\begin{aligned} E(C) &\approx E\left(\sum_{(i,k)\in\Psi_u} \log_2(1 + \gamma_i(k))\right) \\ &\approx N_{\Psi_u} E\left(\log_2(1 + \gamma_i(k))\right), \end{aligned} \tag{31}$$

where $(i, k) \in \Psi_u$.

Combining (6), (7), (23), (25) and (31), $E(C)$ can be further reduced to

$$\begin{aligned} E(C) &\approx N_{\Psi_u} E\left(\log_2(1 + \left(\lambda - \frac{1}{y_i(k)}\right) y_i(k))\right) \\ &\approx N_{\Psi_u} E\left(\log_2(\lambda y_i(k))\right). \end{aligned} \tag{32}$$

Note that (i, k) in (32) belongs to Ψ_u.However, for $(i, k) \in \Psi_u$, the joint PDF of $|H_i(k)|^2$ and Ω_i is not simply determined by the product of (27) and (28). For the convenience of discussion, we define a threshold y_{th} for $y_i(k)$. For any arbitrary $(i_0, k_0) \in \Psi$, if $y_i(k)$ is greater than y_{th}, (i_0, k_0) belongs to Ψ_u. Otherwise, $(i_0, k_0) \in \overline{\Psi}_u$. Thereby, the expected capacity can be computed as

$$\begin{aligned} E(C) \approx N_{\Psi_u} \int_0^{+\infty}\int_0^{+\infty} f_{|H_i(k)|^2}\left(|H_i(k)|^2\right) f_{\Omega}(\Omega_i) \\ \cdot d|H_i(k)|^2 d\Omega_i. \end{aligned} \tag{33}$$

However, the above result is still overly complicated. It is rather challenging to derive the varying threshold due to the randomness of y_{th}. As a result, it is necessary to find a different way to obtain the channel capacity.

B. Approximate Results Using the Central-Limit Theorem

To achieve an approximate solution, the Central-Limit Theorem is resorted to [38]. For mathematical convenience, let $x_k = \sum_{i=1}^{N_{AE}} r_i(k) = \sum_{i=1}^{N_{AE}} \frac{1}{\sigma_n^2}\left(P_i(k)\Omega_i|H_i(k)|^2\right)$, representing the combined SNR of the k-th subcarriers of all the AEs. Since the diversity gain is achieved by using different AEs and multiplexing is realized by different sub-carriers, x_k can be regarded as the combined SNR to achieve the spatial diversity for a given subcarrier k. According to the Central-Limit Theorem, x_k ought to be a Gaussian variable when N_{AE} is large enough. However, the PDF of x_k should be normalized by the probability $p(x_k > 0)$, Thus, the PDF $f_x(x_k)$ is obtained as

$$f_x(x_k) = \begin{cases} \frac{1}{\sqrt{2\pi}\varsigma_k} \exp\left(-\frac{(x_k-\varphi_k)^2}{2\varsigma_k^2}\right)/Q(-\varphi_k/\varsigma_k) & , x_k \geq 0 \\ 0 & , x_k < 0 \end{cases}, \tag{34}$$

where φ_k and ς_k^2 are the mean and variance of x_k prior to normalization, respectively.

Then the expected channel capacity becomes

$$E(C) = E\left(\sum_{k=0}^{N_c-1} \log_2(1 + x_k)\right). \tag{35}$$

There are still N_c integrals to solve before obtaining $E(C)$ in (35), which is still overly complicated

Thanks to the independence of the subcarriers, it is easy to see that, for any two distinct integers k_1 and k_2 $(0 \leq k_1, k_2 \leq N_c)$, x_{k_1} is independent of x_{k_2}. Thus $E(C)$ can be reduced to

$$\begin{aligned} E(C) = E\left(\sum_{k=0}^{N_c-1} \log_2(1 + x_k)\right) &\approx \frac{N_{\Psi_u}}{N_{AE}} E\left(\log_2(1 + x_k)\right) \\ &= \frac{N_{\Psi_u}}{N_{AE}} \int_{-\infty}^{+\infty} \log_2(1 + x_k) f_x(x_k)\, dx_k. \end{aligned} \tag{36}$$

Equation (36) suggests a theoretical method to calculate $E(C)$. And φ_k and ς_k^2 are to be obtained via unbiased estimation from statistics.

To obtain an approximate closed-form expression of (36), the Jensen Inequality is utilized. Due to the convexity of $\log(1 + x)$, (36) can be roughly approximated to

$$\begin{aligned} E(C) \approx \frac{N_{\Psi_u}}{N_{AE}} E\left(\log_2(1 + x_k)\right) &\leq \frac{N_{\Psi_u}}{N_{AE}} \log_2(1 + E(x_k)) \\ &= \frac{N_{\Psi_u}}{N_{AE}} \log_2\left(1 + m + \frac{\zeta_k \cdot \exp\left(-\varphi_k^2/2\zeta_k^2\right)}{\sqrt{2\pi} \cdot Q(-\varphi_k/\zeta_k)}\right). \end{aligned} \tag{37}$$

C. Error Probability for the Proposed Scheme

This paper assumes that the same data sequences are transmitted on the same sub-carriers of all the antennas, while different sub-carriers transmit different data sequences. Thus, diversity gains via the antennas are achievable. To overcome the interferences caused by the frequency-selective fading channel, a great deal of work has been done, *i.e.*, rake receiver, frequency-domain equalization (FDE), pre-coding, *etc.*. This paper explores pre-coding methods. Assume that the frequency-domain form of the transmitted signal $s_i(t)$ is given by

$$S_i(k) = d(k) W_i(k), \tag{38}$$

where $d(k)$ is the information sequence with $E[d^2(k)] = 1$, and $W_i(k)$ is the pre-coding weight that is determined by the channel state information as follows

$$W(k) = \frac{H_i^*(k)}{|H_i(k)|} \tag{39}$$

As can be seen from Fig. 2, the received signal $r(t)$ is firstly transformed into the frequency-domain signal $R(k)$ using the FFT, *i.e.*,

$$R(k) = \frac{1}{\sqrt{N_c}} \sum_{t=0}^{N_c-1} r(t) \exp\left(-j2\pi k \frac{t}{N_c}\right) \tag{40}$$

It follows from (1) that

$$R(k) = \sum_{i=1}^{N_{AE}} \left[\sqrt{\Omega_i} H_i(k) \sqrt{P_i(k)} S_i(k)\right] + \Pi(k), \tag{41}$$

where $H_i(k)$ is given by (4). Substituting (38), (39) into (41) gives rise to

$$R(k) = \sum_{i=1}^{N_{AE}} \left[\sqrt{\Omega_i} |H_i(k)| \sqrt{P_i} d_i(k)\right] + \Pi(k). \tag{42}$$

Considering that x_k is defined as $\sum_{i=1}^{N_{AE}} \frac{1}{\sigma_n^2}\left(P_i(k)\Omega_i |H_i(k)|^2\right)$, it is the received SNR of (42). Supposing BPSK is adopted for all the Ψ_u sub-carriers, the BER $P_{e,k}$ of the k-th subcarrier is expressed as

$$P_{e_k} = E\left[Q\left(\sqrt{x_k}\right)\right] = \int_0^{+\infty} Q\left(\sqrt{x_k}\right) f_x(x_k)\, dx_k. \tag{43}$$

Owing to the arbitrariness of k, it is considered that the average BER P_e can be approximated as P_{e_k}. Thus, the total average BER P_e can be calculated as

$$P_e = E\left[P_{e_k}\right] = \frac{1}{N_c} \sum_{k=0}^{N_c-1} \int_0^{+\infty} Q(x_k) f_x(x_k)\, dx_k. \tag{44}$$

As can be inferred from (44), the BER performance improves with the increase of the received SNR.

D. Further Discussions

The probability distribution of C can also be obtained approximately using the above method. Since x_k represents the combined SNR of the k-th subcarriers of the AEs, its value is small, when the total power P is not great. Then (7) becomes

$$C \approx \sum_{k=0}^{N_c-1} \log_2(1 + x_k) \approx \sum_{k=0}^{N_c-1} x_k. \tag{45}$$

TABLE I
SIMULATION PARAMETERS FOR THE DAS

Parameter	Value
Number of paths (L)	16
Number of AEs (N_{AE})	16
Number of sub-carriers (N_c)	128
Shadow fading (σ_i)	8 dB

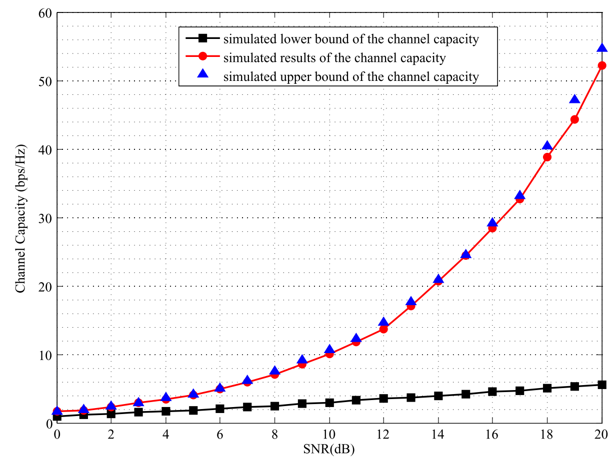

Fig. 4. Upper and lower bounds of the channel capacity.

It is easy to show that the channel capacity C follows a Gaussian distribution, when $x_0, x_1, \cdots, x_{N_c}$ are independent Gaussian variables with a common variance ς_k^2.

Similarly, x_k will be very large when the total power P is extremely large. As a result, (7) becomes

$$C \approx \sum_{k=0}^{N_c-1} \log_2(1 + x_k) \approx \sum_{k=0}^{N_c-1} \log_2(x_k). \tag{46}$$

Thus, C is lognormally distributed, when P is extremely large. In summary, after finding it is intractable to obtain the exact solution to (7), we resorted to the Central-Limit Theorem to derive an approximate solution to the power allocation problem in (25).

V. SIMULATION RESULTS

In this section, both theoretical and simulated results are presented to validate the proposed methods. The simulation parameters are shown in Table I. The distance between the MS and AE is normalized, and $\sum_{l=0}^{L-1} |h_{i,l}|^2 = 1$. Since it is assumed in this paper that the total transmit power P is a constant, in the simulation figures, the SNR reflects the total transmit power to noise power ratio $\frac{P}{\sigma_n^2}$, ranging from 0 dB to 20 dB. In our simulations, the classical Jakes fading model is used to model the fading channel for mathematical analysis.

Fig. 4 plots the simulated channel capacity, and the simulated upper and lower bounds of the channel capacity as given in (12).

As shown in Fig. 4, the channel capacity is extremely close to its upper bound. This is because $y_i(k)$ is always small enough such that $\gamma_i(k)$ is always smaller than one. Therefore, δ_{up}

TABLE II
PROPORTION OF $r_i\ (k) > 1$

SNR (dB)	Proportion	SNR (dB)	Proportion
0	0.00410%	11	0.15483%
1	0.00732%	12	0.20752%
2	0.01250%	13	0.27251%
3	0.01338%	14	0.28696%
4	0.01494%	15	0.39893%
5	0.02905%	16	0.49268%
6	0.02852%	17	0.60190%
7	0.05347%	18	0.72095%
8	0.07036%	19	0.86377%
9	0.10054%	20	1.04922%
10	0.10952%		

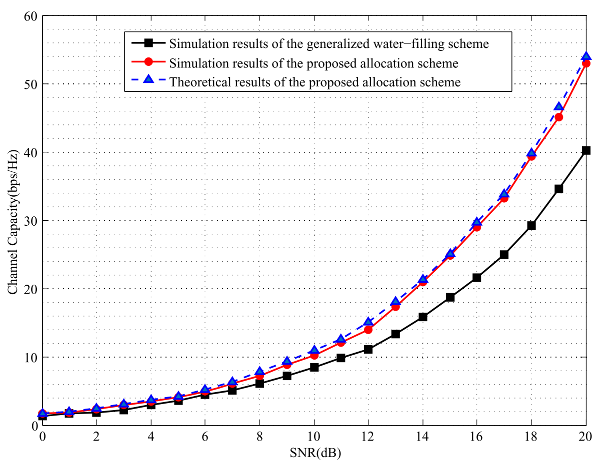

Fig. 5. Performance of the near-optimal scheme.

in (14) is close to zero. The results can be found in Table II, which lists the simulated proportion of $r_i\ (k) > 1$ on all the available subcarriers.

As can be seen from Table II, the proportion of $r_i\ (k) > 1$ is small enough to be negligible, so that δ_{up} approaches zero. It is easy to see from the table that this proportion increases with the SNR, because $P_i\ (k)$ grows with the SNR for any $(i, k) \in \Psi_u$.

As discussed in Section III, it can be found that the lower bound is very loose, since δ_{low} in (17) is approximately zero, if and only if $\sum_{i=1}^{N_{AE}} \gamma_i (k) < 1$. The order of magnitude of $\sum_{i=1}^{N_{AE}} \gamma_i (k)$ can be roughly estimated as $N_{AE} E\ (\gamma_i\ (k))\ \ E\ (\gamma_i\ (k))$. It is easy to see that when the SNR is small, the lower bound is acceptable. However, with the increase of the SNR, the lower bound becomes increasingly inaccurate.

Fig. 5 shows the theoretical and simulated results of the channel capacity. As can be observed from this figure, both the theoretical and simulated results of the near-optimal scheme are approximately identical. The theoretical result is computed by (37), with φ_k and ς_k^2 obtained via unbiased estimation through computing statistics. The unbiased estimates are given in Table III.

One can also infer from Fig. 4 that the difference between the theoretical and simulated results becomes slightly larger when the SNR is greater than 10 dB, since more $\gamma_i\ (k)$ satisfy the condition of $\gamma_i\ (k) > 1$ (as shown in Table II). Actually, the proportion is still small enough to be acceptable.

TABLE III
UNBIASED ESTIMATES OF φ_k AND ς_k^2

SNR (dB)	φ_k	ς_k^2
0	0.200147379	0.057452297
1	0.215953615	0.067923085
2	0.243820885	0.090118114
3	0.271103557	0.108936138
4	0.291560245	0.123939419
5	0.31908522	0.146874036
6	0.353265297	0.188421631
7	0.382579696	0.221689088
8	0.41822711	0.306001697
9	0.456778137	0.347800213
10	0.483423521	0.380850737
11	0.527410295	0.453482652
12	0.578551351	0.580466779
13	0.634739161	0.796129007
14	0.681045054	0.840071177
15	0.751387508	1.116644114
16	0.803034636	1.33170258
17	0.905777359	1.711955922
18	0.972492902	1.911411841
19	1.08773995	2.66618654
20	1.191416751	3.401935006

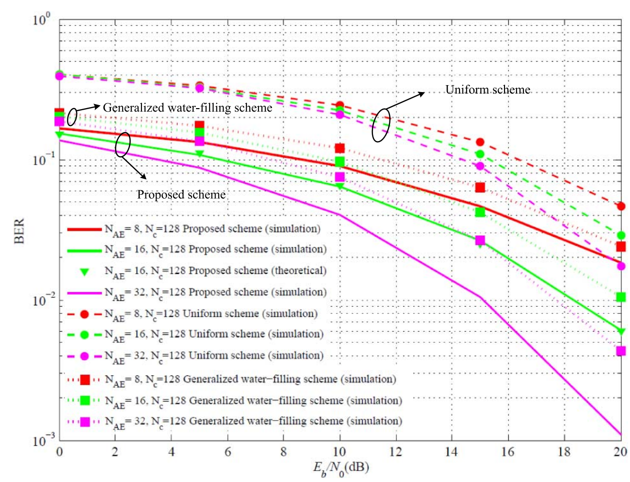

Fig. 6. BER performance in water-filling scheme and uniform allocation scheme.

It can be seen from Fig. 4 and 5 that the near-optimal scheme approaches the upper bound of the capacity closely. Moreover, the channel capacity of our proposed scheme is better than that of the generalized-water filling scheme in [28].

The BER performance of the proposed scheme is plotted in Fig. 6, which is compared with the uniform scheme and the generalized water-filling scheme in [28]. Generally speaking, the BER of the proposed scheme is better than those of the water-filling and uniform allocation schemes, since the received SNR $\gamma_i\ (k)$ of the k-th subcarrier is larger than in the other two schemes. For the uniform allocation case, deep fading leads to more errors. The sub-carriers with poor CSI may be abandoned in the proposed scheme. For the purpose of fairness, suppose each symbol has the same transmit power, which satisfies $(i, j) \in \Psi_u$. It is found that the average number of sub-carriers used approaches N_c, when E_b/N_0 is greater than 10 dB. In Fig. 6, it is shown that the BER slopes approximately equates to the number of AEs, since the diversity orders of the three schemes are all N_{AE}. It is also found that the the slopes of the BER curves with the same color are almost identical, indicating that the diversity gains of the three schemes are nearly identical when N_{AE} is a constant number. Furthermore, the BER performances of all theses schemes improve with the increase of N_{AE}. In summary, the water-filling method is able to reap power gains at the MS, and thus leads to an improved BER performance.

VI. Conclusion

This paper investigated the channel capacity of the DAS over a multi-path frequency-selective fading channel, under the condition that the phase of the channel is unknown to the AEs. After revealing that it is unrealistic to achieve optimal power allocation, the upper and lower bounds of the channel capacity were derived. A near-optimal solution was then proposed through maximizing the upper bound. It was shown that the channel capacity is extremely close to its upper bound through presenting both theoretical and simulated results. The Central-Limit Theorem was utilized to derive the theoretical results and the BER performance was presented for the proposed scheme.

Appendix A

Lemma 1: Providing $a_i > 0$ for any positive integer i, the following holds

$$\prod_{i=1}^{n}(1+a_i) = (1+\sum_{i_1=1}^{n} a_i + \sum_{i_1\neq i_2}^{n} a_{i_1}a_{i_2} + \cdots + \sum_{i_1\neq i_2\neq\cdots i_n}^{n} a_{i_1}a_{i_2}\cdots a_{i_n}), \quad (1)$$

where i_k is a positive integer satisfying $1 \le i_k \le n$ for any integer k.

Proof: We resort to mathematical induction to prove Lemma 1, which consists of two steps. Step one is to prove that the case of $n = 2$ is correct, while step two is to prove that the case of $n = t$ (t is an integer larger than 2) is correct.

Step one: when $n = 2$, it is easy to show that

$$\prod_{i=1}^{2}(1+a_i) = (1+\sum_{i=1}^{2} a_i + a_1a_2). \quad (2)$$

Step two: supposing that (1) is true, when $n = t$ and t is an integer larger than 2, we arrive at

$$\prod_{i=1}^{t}(1+a_i) = 1+\sum_{i_1=1}^{t} a_i + \sum_{i_1\neq i_2}^{t} a_{i_1}a_{i_2} + \cdots + \sum_{i_1\neq i_2\neq\cdots i_t}^{t} a_{i_1}a_{i_2}\cdots a_{i_t}. \quad (3)$$

Then if $n = t + 1$ and due to (3), it follows

$$\begin{aligned}
&\prod_{i=1}^{t+1}(1+a_i) = \\
&(1+\sum_{i_1=1}^{t} a_i + \cdots + \sum_{i_1\neq i_2\neq\cdots i_t}^{t} a_{i_1}a_{i_2}\cdots a_{i_t})\,(1+a_{t+1}) \\
&= 1+\sum_{i_1=1}^{t} a_i + \cdots + a_{t+1}\sum_{i_1\neq i_2\neq\cdots i_{t-1}}^{t-1} a_{i_1}a_{i_2}\cdots a_{i_{t-1}} \\
&+ \sum_{i_1\neq i_2\neq\cdots i_t}^{t} a_{i_1}a_{i_2}\cdots a_{i_t} + \sum_{i_1\neq i_2\neq\cdots i_{t+1}}^{t+1} a_{i_1}a_{i_2}\cdots a_{i_{t+1}} \\
&= 1+\sum_{i_1=1}^{t+1} a_i + \cdots + \sum_{i_1\neq i_2\neq\cdots i_{t+1}}^{t+1} a_{i_1}a_{i_2}\cdots a_{i_{t+1}}. \quad (4)
\end{aligned}$$

Thereby, eqn. (1) is correct when $n = t + 1$. According to mathematical induction, Lemma 1: is thus proved. ■

Appendix B

Lemma 2: Providing $a_i > 0$ for any positive integer i, the following holds

$$\log_2(1+\sum_{i=1}^{n} a_i) < \sum_{i=1}^{n}\log_2(1+a_i). \quad (1)$$

Proof: We resort to mathematical induction to prove Lemma 2, which consists of two steps. Step one is to prove that the case of $n = 2$ is correct, while step two is to prove that the case of $n = t$ (t is an integer larger than 2) is correct.

Step one: when $n = 2$, it is easy to show that

$$\begin{aligned}
\log_2(1+\sum_{i=1}^{2} a_i) &< \log_2(1+a_1+a_2+a_1a_2) \\
&= \log_2[(1+a_1)(1+a_2)] \\
&= \log_2(1+a_1)+\log_2(1+a_2) \\
&= \sum_{i=1}^{2}\log_2(1+a_i). \quad (2)
\end{aligned}$$

Step two: supposing that inequality (1) is true, when $n = t$ and t is an integer greater than 2, we arrive at

$$\log_2(1+\sum_{i=1}^{t} a_i) < \sum_{i=1}^{t}\log_2(1+a_i). \quad (3)$$

Then, when $n = t + 1$ and due to (3), it can be shown that

$$\begin{aligned}\log_2\left(1+\sum_{i=1}^{t+1}a_i\right) &= \log_2\left(1+\sum_{i=1}^{t}a_i + a_{t+1}\right)\\ &< \log_2\left(1+\sum_{i=1}^{t}a_i + a_{t+1} + a_{t+1}\cdot\sum_{i=1}^{t}a_i\right)\\ &< \log_2\left[\left(1+\sum_{i=1}^{t}a_i\right)(1+a_{t+1})\right]\\ &< \sum_{i=1}^{t}\log_2(1+a_i) + \log_2(1+a_{t+1})\\ &= \sum_{i=1}^{t+1}\log_2(1+a_i). \qquad (4)\end{aligned}$$

Therefore, inequality (1) is true when $n = t + 1$. According to mathematical induction, Lemma 2 is thus proved. ■

References

[1] G. Wu, C. Yang, S. Li, and Y. Li, "Recent advances in energy-efficient networks and their application in 5G systems," *IEEE Wireless Commun.*, vol. 22, no. 2, pp. 145–151, Apr. 2015.

[2] C. Zhang, S. L. Ariyavisitakul, and M. Tao, "LTE-advanced and 4G wireless communications," *IEEE Commun. Mag.*, vol. 50, no. 2, pp. 102–103, Feb. 2012.

[3] Q. Li *et al.*, "MIMO techniques in WiMAX and LTE: A feature overview," *IEEE Commun. Mag.*, vol. 48, no. 5, pp. 86–92, May 2010.

[4] Y. Okumura, "Field strength and its variability in VHP and UHF land-mobile radio-services," *Rev. Elect. Commun. Lab.*, vol. 16, pp. 825–873, Sep. 1968.

[5] J. D. Parsons, *The Mobile Radio Propagation Channel*. Hoboken, NJ, USA: Wiley, 2000.

[6] S. R. Saunders, *Antennas and Propagation for Wireless Communication Systems*. Hoboken, NJ, USA: Wiley, 1999.

[7] R. Wonil and A. Paulraj, "MIMO channel capacity for the distributed antenna," in *Proc. IEEE Veh. Technol. Conf. (VTC)*, Vancouver, BC, Canada, May 2002, pp. 706–709.

[8] T. Koike-Akino, A. F. Molisch, C. Duan, Z. Tao, and P. Orlik, "Capacity, MSE and secrecy analysis of linear block precoding for distributed antenna systems in multi-user frequency-selective fading channels," *IEEE Trans. Commun.*, vol. 59, no. 3, pp. 888–900, Mar. 2011.

[9] S. Lee, S. Moon, J. Kim, and I. Lee, "Capacity analysis of distributed antenna systems in a composite fading channel," *IEEE Trans. Wireless Commun.*, vol. 11, no. 3, pp. 1076–1086, Mar. 2012.

[10] H. Matsuda, R. Matsukawa, T. Obara, K. Takeda, and F. Adachi, "Channel capacity of distributed antenna network using spacetime block coded-joint transmit/receive diversity," in *Proc. IEEE Int. Conf. Commun. Syst. (ICCS)*, Singapore, Nov. 2010, pp. 559–563.

[11] N. Seifi, A. Wolfgang, and T. Ottosson, "Downlink performance and capacity of distributed antenna systems based on realistic channel model," in *Proc. Int. ITG Workshop Smart Antennas (WSA)*, Darmstadt, Germany, Feb. 2008, pp. 249–253.

[12] J. Wang, J. Wang, X. Dang, M. Lin, Y. Jiao, and M. Chen, "System capacity analysis of downlink distributed antenna systems over composite channels," in *Proc. IEEE Int. Conf. Commun. Technol. (ICCT)*, Nanjing, China, Nov. 2010, pp. 1076–1079.

[13] H. Chen and M. Chen, "Capacity of the distributed antenna systems over shadowed fading channels," in *Proc. IEEE Veh. Technol. Conf. (VTC)*, Barcelona, Spain, Apr. 2009, pp. 1–4.

[14] J. Zhang, C. Wen, S. Jin, X. Gao, and K. Wong, "On capacity of large-scale MIMO multiple access channels with distributed sets of correlated antennas," *IEEE J. Sel. Areas Commun.*, vol. 31, no. 2, pp. 133–148, Feb. 2013.

[15] S. A. Ahmadi and H. Yanikomeroglu, "The ergodic and outage capacities of distributed antenna systems in generalized-K fading channels," in *Proc. IEEE 21st Int. Symp. Pers. Indoor Mobile Radio Commun. (PIMRC)*, Istanbul, Turkey, Sep. 2010, pp. 662–666.

[16] C. Xiu, Q. Zhang, J. Wang, and J. Liu, "Capacity of Gaussian vector multiple access channels with distributed antennas," in *Proc. Int. Conf. ITS Telecommun.*, Chengdu, China, Jun. 2006, pp. 541–544.

[17] J. Park, E. Song, and W. Sung, "Capacity analysis for distributed antenna systems using cooperative transmission schemes in fading channels," *IEEE Trans. Wireless Commun.*, vol. 8, no. 2, pp. 586–592, Feb. 2009.

[18] A. Lapidoth and S. M. Moser, "Capacity bounds via duality with applications to multiple-antenna systems on flat-fading channels," *IEEE Trans. Inf. Theory*, vol. 49, no. 10, pp. 2426–2467, Oct. 2003.

[19] L. Dai, "A comparative study on uplink sum capacity with co-located and distributed antennas," *IEEE J. Sel. Areas Commun.*, vol. 29, no. 6, pp. 1200–1213, Jun. 2011.

[20] T. H. Pham and R. Kohno, "Bound of capacity in distributed MIMO repeater system with AF method," in *Proc. IEEE Int. Conf. Commun. Signal Process. (ICCSP)*, Kerala, India, Feb. 2011, pp. 75–79.

[21] Z. Ye, L. Sun, Q. Yu, and Z. Zhang, "Capacity analysis of downlink MRT-SC in distributed antenna system," in *Proc. IEEE Chinacom*, Harbin, China, Aug. 2011, pp. 330–334.

[22] W. Feng, Y. Li, S. Zhou, and J. Wang, "Downlink power allocation for distributed antenna systems in a multi-cell environment," in *Proc. IEEE WiCom*, Beijing, China, Sep. 2009, pp. 1–4.

[23] Y. Wang, W. Feng, Y. Zhao, S. Zhou, and J. Wang, "Joint power allocation for multi-cell distributed antenna systems with large-scale CSIT," in *Proc. IEEE Int. Conf. Commun. (ICC)*, Ottawa, ON, Canada, Jun. 2012, pp. 5264–5269.

[24] D. Lim, K. Choi, and H. Liu, "Optimum power allocation for distributed antenna systems with large-scale fading-only feedback," in *Proc. IEEE 6th Int. Conf. Inf. Technol. New Gener. (ITNG)*, Las Vegas, NV, USA, Apr. 2009, pp. 1158–1164.

[25] W. Feng, X. Zhang, S. Zhou, J. Wang, and M. Xia, "Downlink power allocation for distributed antenna systems with random antenna layout," in *Proc. IEEE Veh. Technol. Conf. (VTC)*, Barcelona, Spain, Apr. 2009, pp. 1–5.

[26] X. Chen, X. Xu, and X. Tao, "Energy efficient power allocation in generalized distributed antenna system," *IEEE Commun. Lett.*, vol. 16, no. 7, pp. 1022–1025, Jul. 2012.

[27] L. Tian, Y. Zhou, Y. Zhang, G. Sun, and J. Shi, "Power and subcarrier allocation for multicast services in distributed antenna systems," in *Proc. IEEE GLOBECOM*, Houston, TX, USA, Dec. 2011, pp. 1–5.

[28] G. Scutari and S. Barbarossa, "Generalized water-filling for multiple transmit antenna systems," in *Proc. IEEE Int. Conf. Commun. (ICC)*, Anchorage, AK, USA, May 2003, pp. 2668–2672.

[29] H. Kim, S.-R. Lee, C. Song, K.-J. Lee, and I. Lee, "Optimal power allocation scheme for energy efficiency maximization in distributed antenna systems," *IEEE Trans. Commun.*, vol. 63, no. 2, pp. 431–440, Feb. 2015.

[30] Y. Li, M. Sheng, X. Wang, Y. Shi, and Y. Zhang, "Globally optimal antenna selection and power allocation for energy efficiency maximization in downlink distributed antenna systems," in *Proc. IEEE GLOBECOM*, Dec. 2014, pp. 3856–3861.

[31] J. Wu, J. Liu, W. Li, and X. You, "Low-complexity power allocation for energy efficiency maximization in DAS," *IEEE Commun. Lett.*, vol. 19, no. 6, pp. 925–928, Jun. 2015.

[32] H. Zhu and J. Wang, "Radio resource allocation in multiuser distributed antenna systems," *IEEE J. Sel. Areas Commun.*, vol. 31, no. 10, pp. 2058–2066, Oct. 2013.

[33] P. Gong, K. Yu, and Y. Wang, "Radio resource allocation for multiuser OFDMA distributed antenna systems," in *Proc. IEEE Int. Conf. Netw. Infrastruct. Digital Content (IC-NIDC)*, Nov. 2009, pp. 912–916.

[34] L. Cheng, Y. Gao, Y. Li, D. Yang, and X. Liu, "A cooperative resource allocation scheme based on self-organized network in ultra-dense small cell deployment," in *Proc. IEEE Veh. Technol. Conf. (VTC-Spring)*, May 2015, pp. 1–6.

[35] J. Yan, J. Li, and L. Zhao, "Joint user schedulilng and power allocation with quality of service guarantees in downlink distributed antennas system," *IET Commun.*, vol. 8, no. 3, pp. 299–307, Feb. 2014.

[36] X. Zhang and Y. Sun, "Distributed power allocation for coordinated multipoint transmissions in distributed antenna systems," *IEEE Trans. Wireless Commun.*, vol. 12, no. 5, pp. 2281–2291, May 2013.

[37] Q. Yu, W. Meng, and F. Adachi, "Two-dimensional block-spread CDMA relay using virtual four antenna STCDTD," *IEEE Trans. Veh. Technol.*, vol. 62, no. 8, pp. 3813–3827, Oct. 2013.

[38] J. R. Proakis, *Digital Communication*. New York, NY, USA: McGraw-Hill, 2009.

[39] T. M. Cover and A. A. El-Gamal, "Capacity theorems for the relay channel," *IEEE Trans. Inf. Theory*, vol. 25, no. 5, pp. 572–584, Sep. 1979.

[40] T. M. Cover and J. A. Thomas, *Information Theory*. New York, NY, USA: Wiley-Interscience, 2006.

Qi-Yue Yu (M'10) received the B.S., M.S., and Ph.D. degrees in communications engineering from Harbin Institute of Technology (HIT), Harbin, China, in 2004, 2006, and 2010, respectively. She is currently an Associate Professor with the School of Electronics and Information Engineering, HIT. From April 2007 to March 2008, she studied with the Adachi Lab, Tohoku University, Japan, as a Research Assistant of the Tohoku University Global COE Program. In 2010, she was invited to visit the City University of Hong Kong, and to visit University of Southern Queensland in 2014. She is currently a Visiting Scholar at the University of California at Davis, Davis, CA, USA, from September 2015 to September 2016. Her research interests include modulation and coding, multi-access techniques, and MIMO for broadband wireless communications.

Ya-Tian Li received the B.S. and M.S. degrees in communications engineering from Harbin Institute of Technology (HIT), Harbin, China, in 2013 and 2015, respectively. He is currently a Research Assistant with the Changchun Institute of Optics, Fine Mechanics and Physics (CIOMP), Chinese Academy of Sciences, Changchun, China. His research interests include wireless communications and free space optics.

Wei Xiang (S'00–M'04–SM'10) received the B.Eng. and M.Eng. degrees, both in electronic engineering, from the University of Electronic Science and Technology of China, Chengdu, China, and the Ph.D. degree in telecommunications engineering from the University of South Australia, Adelaide, S.A., Australia, in 1997, 2000, and 2004, respectively. He is currently a Professor and the Program Director with the College of Science, Technology and Engineering, James Cook University, Cairns, Australia. From 2004 to 2015, he was an Associate Professor with the School of Mechanical and Electrical Engineering, University of Southern Queensland, Toowoomba, Qld., Australia. In 2008, he was a Visiting Scholar at Nanyang Technological University, Singapore. From 2010 to 2011, he was a Visiting Scholar at the University of Mississippi, Oxford, MS, USA. From 2012 to 2013, he was an Endeavour Visiting Associate Professor at the University of Hong Kong. In 2015, he was a Visiting Scholar at the University Tsukuba, Japan. His research interests include communications and information theory, particularly coding and signal processing for multimedia communications systems. He is an IET Fellow. He was the recipient of several prestigious fellowship titles, including a Queensland International Fellow (2010–2011) by the Queensland Government of Australia, an Endeavour Research Fellow (2012–2013) by the Commonwealth Government of Australia, a Smart Futures Fellow (2012–2015) by the Queensland Government of Australia, and a JSPS Invitational Fellow jointly by the Australian Academy of Science and Japanese Society for Promotion of Science (2014–2015). He was a co-recipient of the Best Paper Awards at 2015 WCSP and 2011 IEEE WCNC.

Wei-Xiao Meng (SM'10) received the B.Eng., M.Eng., and Ph.D. degrees from Harbin Institute ofTechnology (HIT), Harbin, China, in 1990, 1995, and 2000, respectively. From 1998 to 1999, he worked at NTT DoCoMo on adaptive array antenna and dynamic resource allocation for beyond 3G as a senior visiting researcher. He is now a Full Professor with the School of Electronics and Information Engineering of HIT. He has authored three books and over 200 papers on journals and international conferences. His research interests include broadband wireless communications and networking, MIMO, GNSS receiver, and wireless localization technologies. He is the Chair of IEEE Communications Society Harbin Chapter, a Senior Member of IET, the China Institute of Electronics, and the China Institute of Communication. He has been an Editorial Board Member for *Wireless Communications and Mobile Computing (Wiley)* since 2010, an Area Editor for *Physical Communication (Elsevier)* since 2014, and an Editorial Board member for IEEE COMMUNICATIONS SURVEYS AND TUTORIALS. He served as leading TPC Co-Chair of ChinaCom2011, leading Services and Applications Track Co-Chair of the IEEE WCNC2013, Awards Co-Chair of the IEEE ICC2015 and Wireless Networking Symposia Co-Chair of GLOBECOM 2015. In 2005, he was honored provincial excellent returnee and selected into New Century Excellent Talents (NCET) plan by the Ministry of Education, China, in 2008.

Wen-Yan Tang received the B.S. and M.S. degrees in precision instruments and machinery from Harbin Institute of Technology (HIT), Harbin, China, and the Ph.D. degree in mechanical engineering from the University of Kaiserslautern, Kaiserslautern, Germany, in 1982, 1984, and 1990, respectively. His research interests include precision instrument and control, and communications system control.